AT&T BELL LABORATORIES TECHNICAL JOURNAL
Vol. 63, No. 4, April 1984
Printed in U.S.A.

BER Degradations Caused by Switching in Digital Mobile Radio Systems Using Base Station Diversity

By B. S. GLANCE*

(Manuscript received August 3, 1983)

This paper presents a study of the Bit Error Rate (BER) degradation resulting from base station switching in digital mobile radio systems using base station diversity to combat shadow fading. The degradation is caused by the discontinuities of the signal received by the mobile unit when transmission is switched from one base station to another. To evaluate this effect, a simple statistical model has been devised for the spatial variations of shadow fading. It consists of a one-parameter spatial autocorrelation function for the (Gaussian) decibel value of the fading loss, which can be easily simulated. The single parameter is a correlation length, which can be varied to emulate different fading conditions in the urban environment. The shape of the autocorrelation function can similarly be varied. This model was used to evaluate the BER degradation of mobile radio systems using Phase-Shift-Keying (PSK) modulation. The results show that, in worst-case conditions, the BER is insignificantly affected by switching for BER values above 9×10^{-5} for two-PSK and 1.5×10^{-4} for four-PSK. Adding a threshold into the switching test can reduce or increase the switching degradation, depending on the threshold value.

I. INTRODUCTION

Shadow fading in mobile radio propagation is caused by large obstacles blocking the transmission path. This effect is combated in cellular systems by using base station diversity.[1] The arrangement consists of several base stations at different locations in the cell, which

*AT&T Bell Laboratories.

provide path diversity. Only one base station transmits to the mobile receiver. Switching tests are done at regularly spaced intervals, Δx, to compare the signals received by the base stations. As the mobile unit moves, the transmission is switched from one base station to another according to the base station receiving the strongest signal.

In mobile radio systems using digital modulation, the signal discontinuities caused by base station switching give rise to transient errors in the recovery of the digital information. The purpose of the present study is to evaluate the degradation of the Bit Error Rate (BER) due to switching in a cellular system using Phase-Shift-Keying (PSK) modulation and three-corner base station diversity.

Section II defines the mobile radio system used for this evaluation. A simple shadow model (including spatial variations) is proposed in Section III to emulate the shadow fading conditions in an urban environment. This model is used in Section IV to determine the statistics of the distance traveled by a mobile unit between consecutive switches. This is done for different mobile paths covering the surface of a cell and for different fading conditions. Section V evaluates the number of errors caused by switching, and Section VI evaluates the BER degradation caused by switching for two-PSK modulation. These calculations are done for different signaling rates, different distances between switching tests, and different fading conditions. The same evaluation is then replicated in Section VII for four-PSK modulation. Finally, Section VIII assesses the effect on the BER of a threshold condition in the switching test.

II. THE MOBILE RADIO SYSTEM

Consider a cellular, digital mobile radio system having a three-frequency reuse plan, and with three base stations per cell located at alternate corners (see Fig. 1). Shadow fading is combated by selecting the base station receiving the strongest mobile signal. This is achieved by periodically comparing the medium-term power of the mobile signals received by the three base stations; the power is measured over a time period adjusted so as to average out the Rayleigh fading.[2]

The power measured by a base station depends on the distance between the mobile receiver and the base station, and on the shadow attenuation affecting that transmission path. The measurement corresponding to the jth path, $j = 1, 2, or\ 3$, can be expressed by

$$\langle S_j \rangle = S_o \frac{L_j}{r_j^{\gamma}}, \tag{1}$$

where r_j is the distance in miles; S_o is the median power received at a distance of one mile; L_j is a random variable with a log-normal distribution, representing the shadow attenuation; and γ is the prop-

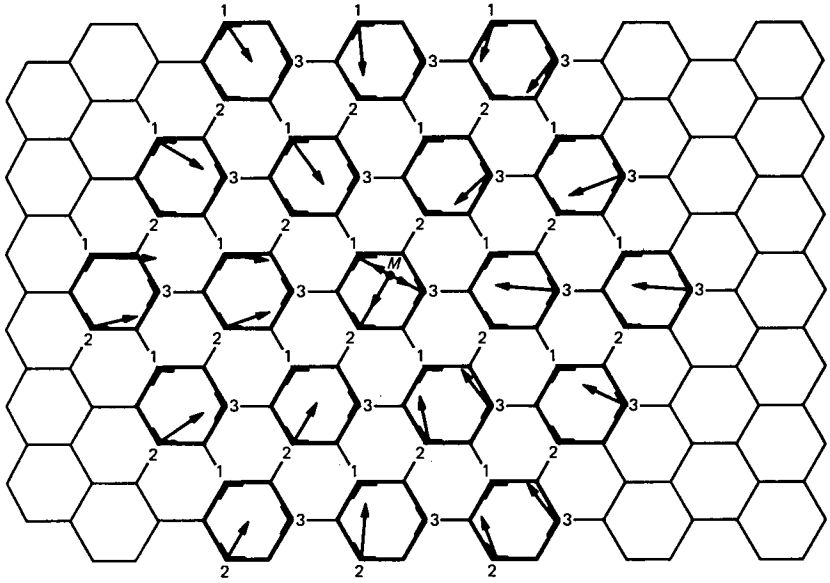

Fig. 1—Three-frequency reuse cellular configuration, with base stations that interfere with desired signal at mobile receiver.

agation law exponent. In our calculations, we assume that γ is 3.8 and that the standard deviation of the Gaussian variable 10 $\log_{10}\{L\}$ is 8 dB.[3,4]

The signal modulation is either two-PSK or four-PSK, with differential encoding. (Differential encoding is required because the mobile receiver cannot retrieve the absolute value of the carrier phase.) The signal at the receiver output of the mobile unit consists of several maximal-ratio-combined space diversity signals, where we assume three branches for two-PSK and four branches for four-PSK. The number of combining branches in each case represents the minimum number required to obtain a medium-term bit error rate $\langle BER \rangle$ below 10^{-3} with 90-percent probability. The combining can be done at both sides of the transmission path or at the base station only by using time-division retransmission;[5] the switching-induced degradation studied here is independent of which scheme is used.

The system performance is assumed to be primarily limited by the interference originating from transmitters using the same radio channel in other cells. Most of the interference comes from the nearest 18 cells[4] (see Fig. 1). The medium-term signal-to-interference ratio ($\langle SIR \rangle$) is given for the jth base station to mobile unit path by

$$\langle SIR_j \rangle = \left(\frac{L_j}{r_j^\gamma}\right) \Big/ \sum_{i=1}^{N} \frac{L_i}{r_j^\gamma} \qquad j = 1, 2, \text{ or } 3. \tag{2}$$

For the reception at the mobile unit, the quantity r_i represents the distance between the ith interfering base station and the mobile unit; L_i is the shadow attenuation of the same path; and N is the number of interfering base stations, a quantity varying between 0 and 18, depending on which base stations are transmitting in the 18 interfering cells. The quantity $\langle BER \rangle$ is a function of $\langle SIR \rangle$ for an uninterrupted base station–mobile radio link. When the base station is switched, additional errors caused by the signal discontinuity increase the $\langle BER \rangle$. The resulting value of $\langle BER \rangle$ thus depends on the switching frequency. For a given mobile unit path, the switching frequency varies according to the position of the mobile unit relative to the three base stations and with the values of the shadow attenuation of the three corresponding paths. A shadow fading model is proposed in the next section for use in calculating this effect.

III. THE SHADOW FADING MODEL

Measurements of the spatial variation of the shadow fading in an urban environment have been reported previously.[6] No statistical analysis has been made for results of this kind. It was therefore decided to represent shadow fading along a mobile unit path by a simple one-dimensional spatial autocorrelation function for the Gaussian random variable $10 \log_{10}\{L\}$, which can be easily simulated. The dependence of the autocorrelation function on the perpendicular direction to the mobile unit path is neglected by assuming a relatively large spacing between parallel paths. The autocorrelation function is characterized by a single parameter, defined as a correlation length, which can be varied to emulate different fading conditions in the urban environment. The same effect is also achieved by changing the shape of the autocorrelation function. This is done in the present study by using two different shapes. The first one, given by

$$\rho_1(x) = e^{-x/x_1}, \tag{3}$$

simulates fading conditions having a relatively fast decorrelation between fades. The second one, given by

$$\rho_2(x) = e^{-x/x_2}(1 + x/x_2), \tag{4}$$

represents fading conditions having a slower decorrelation for distances that are small relative to the decorrelation length. The two constants, x_1 and x_2, are adjusted so that the decorrelation length is the same for both functions, the correlation length being defined as the distance x, which makes both correlation functions decrease to 0.1.

The autocorrelation function $\rho_2(x)$ represents more realistically the spatial variation of shadow fading than does $\rho_1(x)$, which we believe

to be pessimistic because it decays faster near the origin. The shadow fading model is used in the next section to analyze the switching statistics, specifically, the statistics of the distance traveled by a mobile unit between consecutive base station switches.

IV. SWITCHING STATISTICS

The switching statistics are evaluated using a Monte Carlo computer program simulating a mobile receiver moving along a given path covering the entire cell. For simplicity, the simulation is assumed to be statistically stationary for the shadow fading process, including a fixed correlation length over the path. The same calculations are repeated for different values of the correlation length and for the two autocorrelation functions cited above. By assuming an artificial environment (e.g., statistically stationary, with fixed correlation length), but considering different shapes and parameter values, we aim to identify the critical features of the shadow fading process.

The signal received by the mobile unit originates from the base station that received the strongest medium-term power $\langle S_j \rangle$ [see eq. (1)] during the past measurement. A switching test is done after each mobile unit displacement, $\Delta\chi$, to compare the updated value of $\langle S_j \rangle$ to the similar quantities measured by the two other base stations. When $\langle S_j \rangle$ falls below one of the two other measurements, transmission is switched to the base station providing the strongest value. Otherwise, transmission is continued from the same base station until the next test.

The simulation is done for three different mobile unit paths to determine the influence of the path on the switching statistics. The diagonal of the hexagonal cell is taken to be 3000m. The first path is a meander made of parallel lines spaced every $(150\sqrt{3})/2$ meters, starting at base station 2 and directed towards the apex located between base stations 2 and 3 (see Fig. 2a). The second path is also a meander, perpendicular to the first one, starting from the apex located between base stations 1 and 2 and directed towards base station 1 (see Fig. 2b). The third path consists of concentric circles about the cell center, which is the origin of the mobile unit path (see Fig. 2c).

The distributions of the cumulative probability of the distance traveled by the mobile unit between consecutive switches is evaluated for fading conditions having decorrelation lengths of 50, 100, and 200m. This is done in each case for various values of the displacements, Δx. Two significant results emerge. First, the distributions corresponding to different decorrelation lengths can be fitted on the same curves when the distance, x, and the displacement, Δx, are both normalized by the decorrelation length, x_d. Second, the results are almost independent of the path followed by the mobile unit. Both these findings

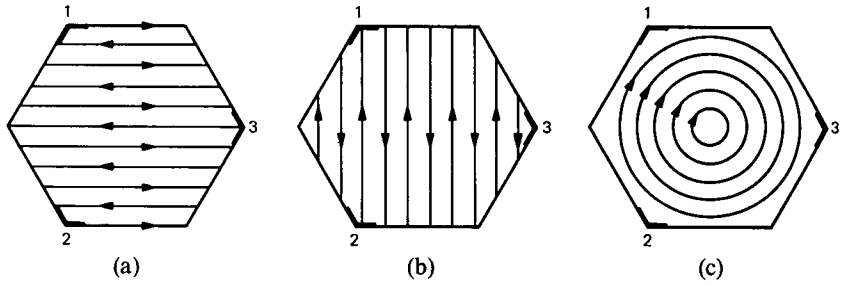

Fig. 2—Three different mobile unit paths used for calculations of switching statistics.

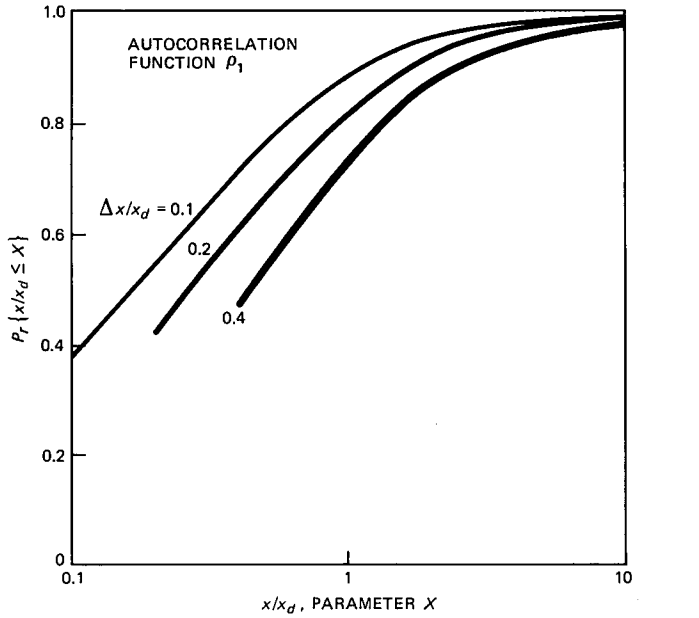

Fig. 3—Cumulative probability distribution of distance traveled by mobile unit between consecutive base station switches, calculated using autocorrelation function ρ_1.

are confirmed by the thickness of the curves in Fig. 3, which represent the spreads due to superimposing results for the three paths and the three decorrelation lengths. Note that the distributions are, however, dependent on the parameter Δx. These curves are all for the autocorrelation function ρ_1, [see (3)].

Similar results are obtained for the autocorrelation function ρ_2 [see (4)], as shown in Fig. 4. In this case, the spread due to the different paths is slightly larger, but the dependence on the parameter Δx is smaller and becomes almost nil for normalized values equal to or below 0.2. This effect is shown in Fig. 5, which compares the distribution

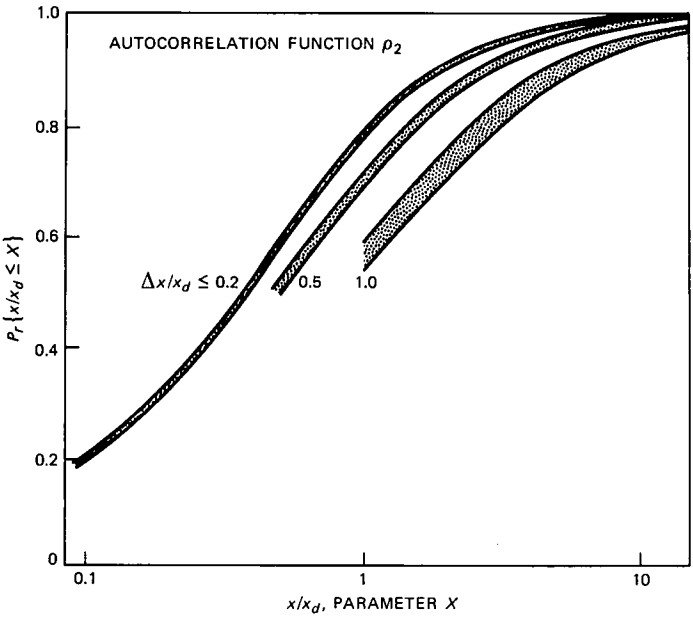

Fig. 4—Same results as in Fig. 3, for the autocorrelation function ρ_2.

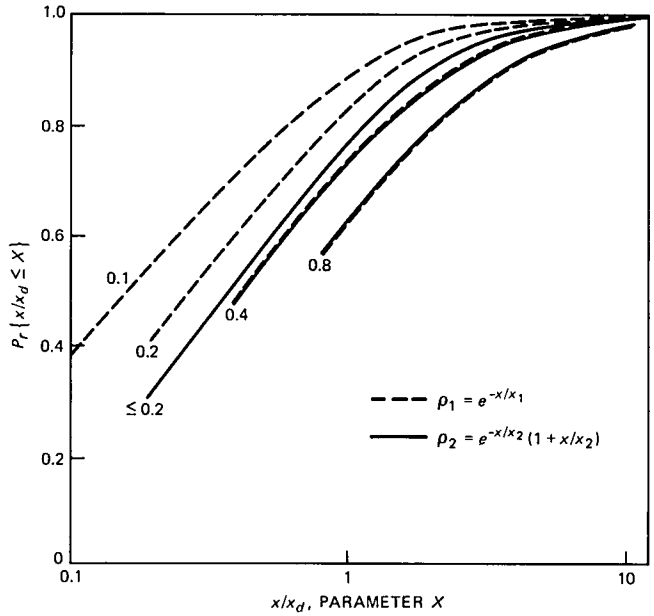

Fig. 5—Comparison between cumulative probabilities obtained with ρ_1 and ρ_2 for same normalized mobile unit displacement values of 0.1, 0.2, 0.4, and 0.8.

obtained for the two autocorrelation functions, calculated for a decorrelation length of 50m and displacements of 5, 10, 20, and 40m. As we expected, the divergence between the distributions is significant for Δx values below 10m, but becomes almost nil when Δx is increased to 20m—a value above which both autocorrelation functions are almost identical. Similar results are observed for the distributions calculated for the longer decorrelation lengths.

Another statistical result of interest is the average distance $\langle x \rangle$ traveled by the mobile unit between switches versus the mobile unit displacement, Δx. This quantity is averaged over all the distances given by the distribution for a given path, correlation function, and decorrelation length. These results corresponding to the autocorrelation functions ρ_1 and ρ_2 are shown, respectively, in Figs. 6 and 7, where

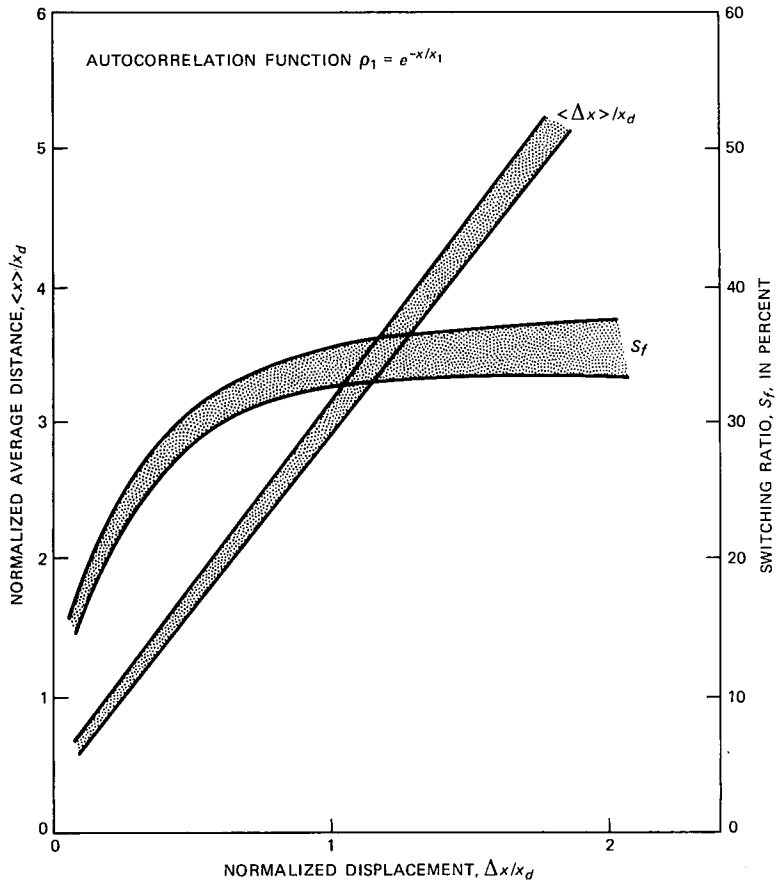

Fig. 6—Average distance and switching frequency versus mobile unit displacement calculated with ρ_1.

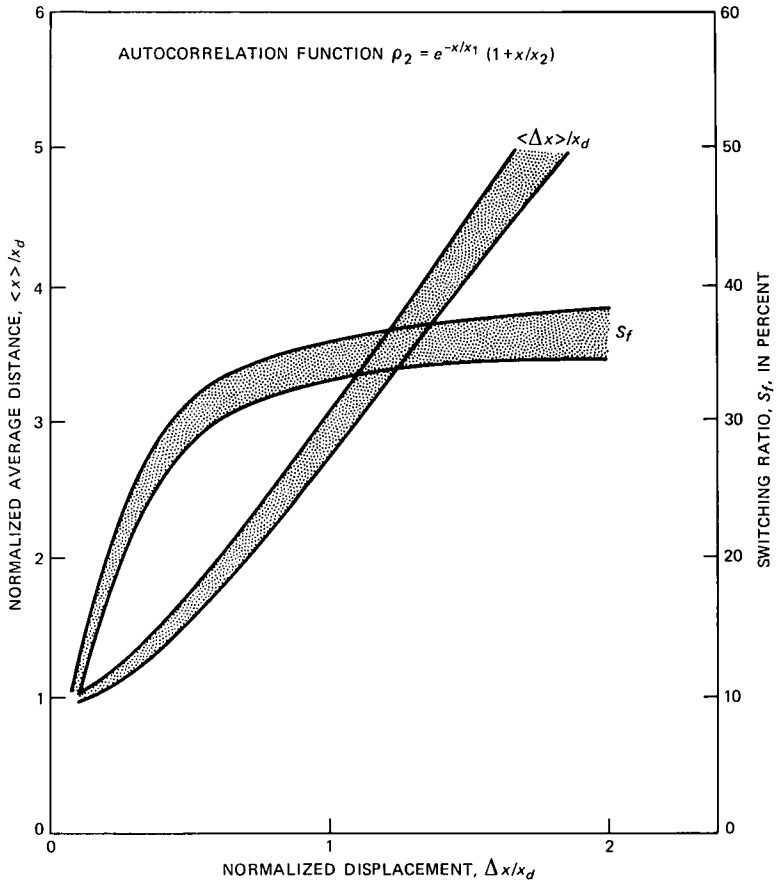

Fig. 7—Same results as for Fig. 6, calculated with ρ_2.

$\langle x \rangle$ and Δx are normalized by x_d. The spread shown by these curves is again due to superimposing the results for the paths and different decorrelation lengths. The other curves shown in these figures represent the switching frequency, measured as the ratio of the number of switches to the total number of tests along the path. Note that the frequency increases to about one third when the displacement is above one decorrelation length. This maximum frequency is equal to that given by random switching between the three base stations. Note also that the switching frequency is substantially reduced only when $\Delta x/x_d < 0.1$, a condition fulfilled for fading distribution having long decorrelation lengths.

V. ERRORS CAUSED BY SWITCHING

Switching between base stations causes phase and amplitude dis-

continuities in the signal received by the mobile unit. These effects generate errors in the demodulation process, in addition to those produced by the interference corrupting the desired signal. The number of switching errors depends on the type of demodulator used for recovering the data. Differential detection, which is only sensitive to phase discontinuities, gives rise, on average, to one-half error per switch because the phase discontinuities are random and uniformly distributed. The switching errors generated by a coherent demodulator lead to a more complex calculation, which depends on the phase and on the amplitude discontinuities.

The amplitude discontinuity is equal to the difference between the instantaneous signal levels received before and after the switch. In the radio mobile environment, these quantities vary randomly over very short distances. Note that the amplitude of the preswitch signal can be larger than that of the postswitch signal, even when the mean value of the latter signal is larger than that of the former. The two instantaneous amplitudes are described by independent random variables having a chi-square distribution of order three for two-PSK signals and order four for four-PSK signals, according to the diversity design defined in Section II.

The number of switching errors is evaluated for a demodulator using "modulation wipeoff" carrier recovery, according to a recently published technique.[7] This is done by assuming that the preswitch and postswitch signals have the same medium-term power and the same medium-term SIR. This approximation is valid when the interval between switching tests is relatively small compared to a decorrelation length. Under these assumptions, one finds that the average number of errors varies between one and two per switch for two-PSK differentially encoded signals, when the $\langle SIR \rangle$ increases from 0 dB to infinity. The same quantity for four-PSK differentially encoded signals varies between 1 and 2.6 errors per switch for the same range of $\langle SIR \rangle$ values (see Fig. 8).

Differential detection thus provides better protection against switching errors. For two-PSK, it also gives nearly the same performance as coherent detection in the absence of switching. For example, the values of $\langle BER \rangle$ given by the differential and coherent detection are, respectively, 4.8×10^{-4} and 3.1×10^{-4} for $\langle SIR \rangle = 9.6$ dB in the case of a three-branch combiner. (The value 9.6 corresponds to the 90-percentile $\langle SIR \rangle$ given by the cellular configuration described in Section II.) This result comes from relations[8]

$$\langle BER \rangle_{2\phi,\mathrm{Dif}} \approx \frac{1}{2} \frac{1}{[1 + \langle SIR \rangle]^3} \tag{5}$$

and

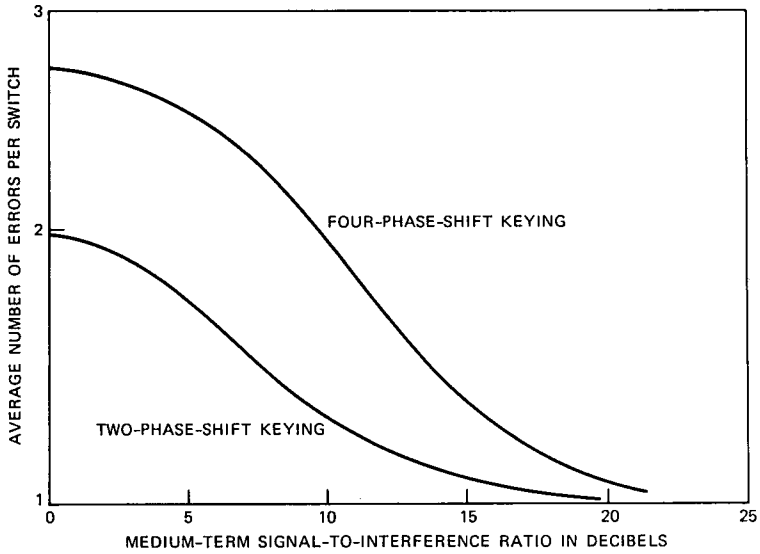

Fig. 8—Average number of switching errors versus $\langle SIR \rangle$, calculated for two-PSK and four-PSK coherently demodulated signals.

$$\langle \mathrm{BER} \rangle_{2\phi,\mathrm{Coh}} = 1 - \sqrt{\frac{\langle SIR \rangle}{1 + \langle SIR \rangle}} \left\{ 1 + \frac{1}{2[1 + \langle SIR \rangle]} + \frac{3}{8[1 + \langle SIR \rangle]^2} \right\}. \quad (6)$$

For four-PSK, on the other hand, differential detection is considerably less efficient than coherent detection. In this case, the $\langle BER \rangle$ expressions (5) and (6), applied to a four-branch combiner, become, respectively,[8]

$$\langle BER \rangle_{4\phi\mathrm{Dif}} \approx \frac{1}{\left[1 + \langle SIR \rangle \left(1 - \frac{1}{\sqrt{2}} \right) \right]^2} \quad (7)$$

and

$$\langle BER \rangle_{4\phi\mathrm{Coh}} = 1 - \sqrt{\frac{\langle SIR \rangle / 2}{1 + \langle SIR \rangle / 2}} \cdot \left\{ 1 + \frac{1}{2\left(1 + \frac{\langle SIR \rangle}{2} \right)} + \frac{3}{8\left(1 + \frac{\langle SIR \rangle}{2} \right)^2} + \frac{15}{48\left(1 + \frac{\langle SIR \rangle}{2} \right)^3} \right\}. \quad (8)$$

The $\langle BER \rangle$ calculated for the same $\langle SIR \rangle$ value is within the required value of 10^{-3} for coherent detection, but it increases to 5.5×10^{-3} for differential detection. In this case, the number of combiner branches would have to be increased by one to fulfill the $\langle BER \rangle$ requirement, a solution which may not be acceptable.

Consequently, the switching-induced degradation of $\langle BER \rangle$ will be computed assuming coherent demodulation for four-PSK signals, and differential detection for two-PSK signals.

VI. PERFORMANCE DEGRADATION DUE TO SWITCHING FOR TWO-PSK

6.1 Calculation of the $\langle BER \rangle$

The degradation is evaluated by comparing the cumulative distributions of $\langle BER \rangle$ obtained with and without switching errors. The distributions are calculated using Monte Carlo simulations, which assume a mobile unit moving along the path shown in Fig. 2a subjected to cochannel interference and shadow fading. (The results are essentially path independent, as noted in Section IV.)

The $\langle BER \rangle$ component due to the interference is calculated every 10m along the mobile unit path according to (5). Switching tests are simulated at regularly spaced intervals, the spacing being a parameter varying from 10m to several times this value. When a switch occurs, the $\langle BER \rangle$ is incremented by

$$\Delta(BER) = \frac{N_e}{S_r} \frac{v}{\delta x}, \tag{9}$$

where N_e represents the number of switching errors, one-half in the present case; S_r is the signaling rate; v is the mobile unit speed; and δx is the distance between $\langle SIR \rangle$ measurements. The calculations are made for the maximum mobile unit speed of 55 mph to obtain conservative estimates of degradation.

The results are first presented for the autocorrelation function ρ_2, which more realistically simulates shadow fading; and for a pessimistic correlation length of 50m, the approximate length of a city block. The results are given for different signaling rates and several values of Δx. The results are then compared to those obtained for longer decorrelation lengths, simulating less severe fading conditions. Finally, the results are also compared to those obtained with the autocorrelation function ρ_1.

6.2 Effect of signaling rate

The cumulative probability distribution was calculated for signaling rates of 16, 32, and 64 kb/s, using the autocorrelation function ρ_2, a correlation length of 50m, and a switching interval of 10m. Figure 9

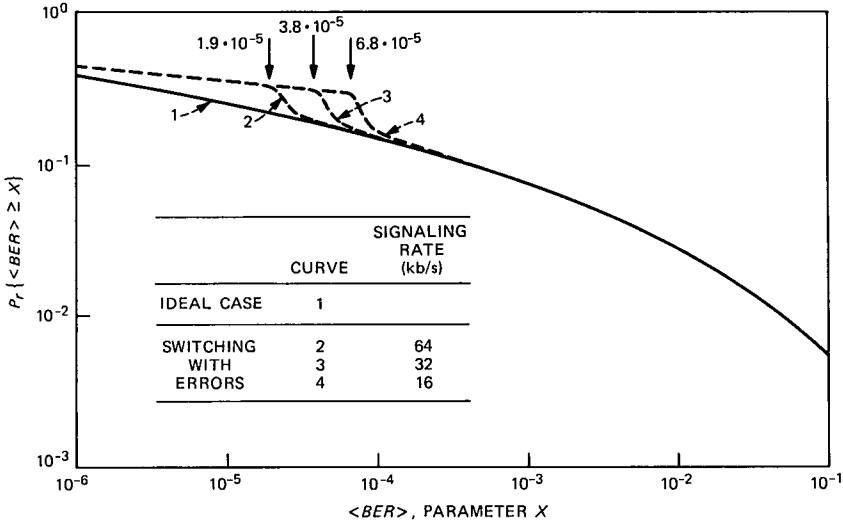

Fig. 9—Cumulative probability of $\langle BER \rangle$ for two-PSK signals, with signaling rate as a parameter.

shows the results and compares them to the ideal case, i.e., a receiver without switching errors. The results show very little switching degradation for $\langle BER \rangle$ values above 10^{-4}. Below this value there is a significant degradation that shifts to lower $\langle BER \rangle$ values when the signaling rate increases. For the above three signaling rates, the rapid change of the distribution begins, respectively, at the $\langle BER \rangle$ values of 6.8×10^{-5}, 3.8×10^{-5}, and 1.9×10^{-5}. These $\langle BER \rangle$ values are almost equal to those given by (9) for the same signaling rates: 7.65×10^{-5}, 3.82×10^{-5}, and 1.9×10^{-5}. At these points, the switching errors increase the cumulative probability by, respectively, 76, 58, and 45 percent.

6.3 Effect of switching interval

Figure 10 shows the cumulative probabilities calculated for the same autocorrelation function, ρ_2, and the same correlation length, 50m, but for different switching intervals, Δx, varying from 10 to 40m. In this case, the signaling rate is 16 kb/s. The results show that the amplitude of the "jump" occurring at the $\langle BER \rangle$ value given by (9) decreases as Δx increases. This effect is explained by noting that the frequency occurrence of the switching tests decreases in inverse proportion to Δx and the resulting degradation decreases accordingly. On the other hand, the use of a large Δx degrades the distribution for the large $\langle BER \rangle$ values because the switching tests are likely to miss the instant at which $\langle S_j \rangle$ [see eq. (1)] falls below that received by one of the two other base stations. This effect increases with the switching

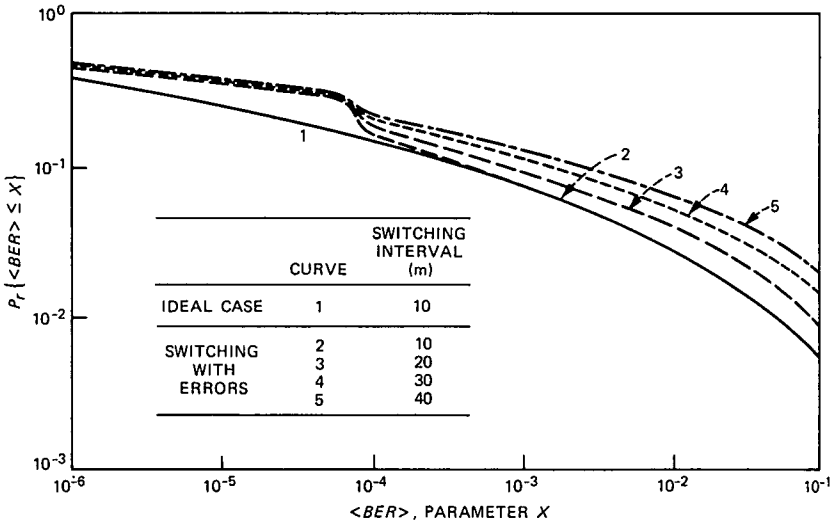

Fig. 10—Cumulative probability of $\langle BER \rangle$ for two-PSK signals, with switching interval as a parameter.

interval. For example, the 90-percentile value of the cumulative probability shifts from a $\langle BER \rangle$ value of 5×10^{-4} to the $\langle BER \rangle$ values of 8×10^{-4}, 1.6×10^{-3}, and 2.5×10^{-3} when the switching interval increases from 10m to, respectively, 20, 30, and 40m.

6.4 Effect of correlation length

Figure 11 illustrates the effect of the correlation length on the cumulative probability distribution of $\langle BER \rangle$. The results are calculated for the autocorrelation function ρ_2, a signaling rate of 16 kb/s, and the correlation lengths of 50, 100, and 200m. The same normalized switching intervals—0.2 and 0.6—are used for the three correlation lengths. As we found previously for the switching statistics, the $\langle BER \rangle$ statistics corresponding to these three correlation lengths fit nearly on the same curve for the same normalized switching interval, except for the section of the distribution on the left of the discontinuity; the amplitude of the discontinuity decreases when the correlation length increases. The explanation of this effect is the same as that given in the previous section.

6.5 Effect of autocorrelation function

The cumulative probabilities obtained with the autocorrelation functions ρ_1 and ρ_2 are compared in Fig. 12. The results correspond to a correlation length of 50m for both functions, a signaling rate of 16 kb/s and the three switching intervals of 10, 20, and 30m. The two

autocorrelation functions give nearly the same distribution for the lowest switching interval value. Above this value, the distributions corresponding to each autocorrelation function diverge increasingly with the length of the switching interval. For example, the 90-percentile point of the cumulative probability shifts from a $\langle BER \rangle$ value of

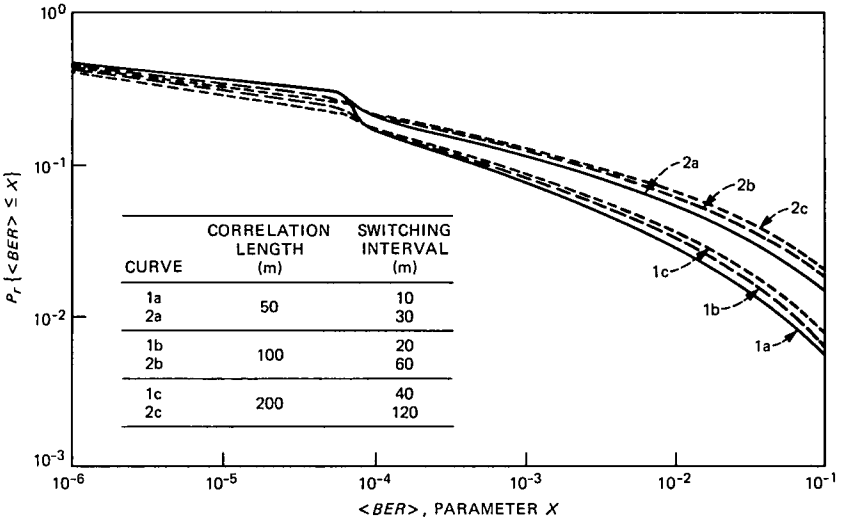

Fig. 11—Cumulative probability of $\langle BER \rangle$ for two-PSK signals, with correlation length as a parameter.

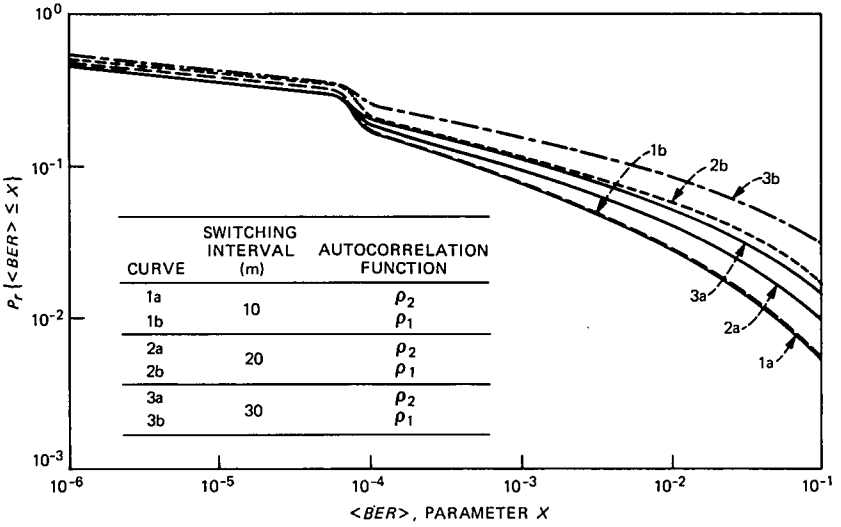

Fig. 12—Cumulative probability of $\langle BER \rangle$ for two-PSK signals, with autocorrelation shape function as a parameter.

8×10^{-4} to 1.8×10^{-3} for a switching interval of 20m, and from of 4.5 $\times 10^{-3}$ to 6×10^{-3} for a switching interval of 30m.

VII. PERFORMANCE DEGRADATION DUE TO SWITCHING FOR FOUR-PSK

The switching degradation for four-PSK is evaluated for coherently detected signals, using the same simulation as for two-PSK. In this case, however, the number of switching errors is given by the relation shown in Fig. 8, and the $\langle BER \rangle$ resulting from the interference is calculated according to (9). The results are presented as functions of the same parameters and for the same conditions as for two-PSK.

7.1 Effect of signaling rate

Cumulative probability distributions were calculated for signaling rates of 16, 32, and 64 kb/s, using the autocorrelation function ρ_2, a correlation length of 50m, and a switching interval of 10m. The results are shown in Fig. 13 and are compared to the ideal case without switching errors. The discontinuities of the distribution are now shifted to higher $\langle BER \rangle$ values, as expected from (9), since the number of switching errors is larger for four-PSK. They occur for the above signaling rates at, respectively, 1.3×10^{-4}, 7×10^{-5}, and 4×10^{-5}. These are about twice the values given for two-PSK.

7.2 Effect of switching interval

The effect of the switching interval is illustrated in Fig. 14, which

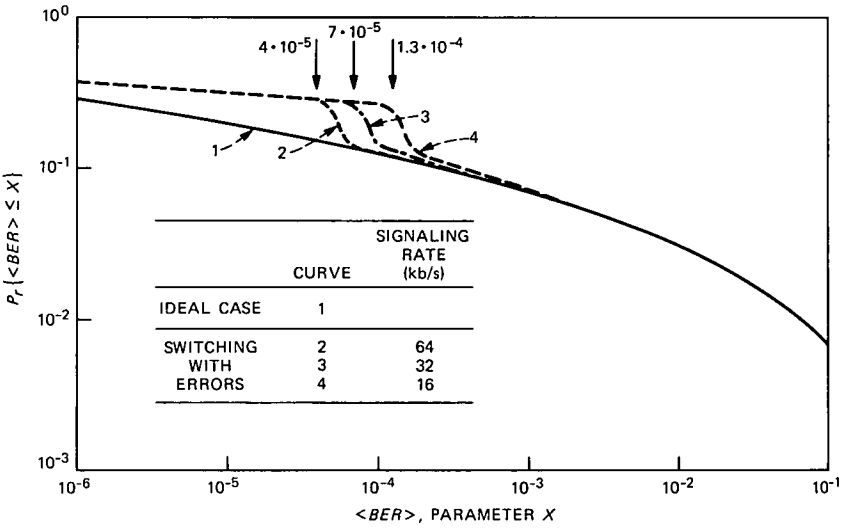

Fig. 13—Same results as in Fig. 9, for four-PSK signals.

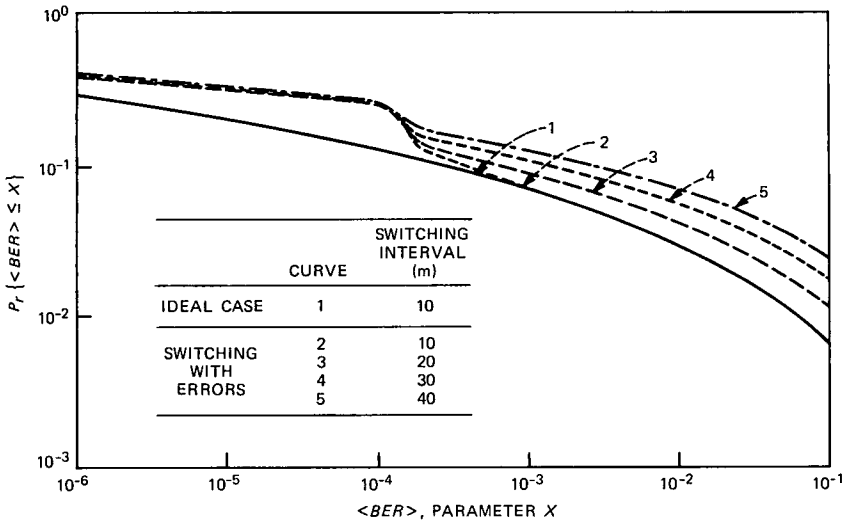

Fig. 14—Same results as in Fig. 10, for four-PSK signals.

gives the cumulative probabilities calculated for intervals varying from 10 to 40m. They are obtained using the autocorrelation function ρ_2, a decorrelation length of 50m, and a signaling rate of 16 kb/s. The effect of the switching interval is essentially the same as that found for two-PSK. The differences are that the discontinuities are shifted to higher $\langle BER \rangle$ values, as previously discussed, and the cumulative probability increases at this point by 100 percent (instead of 76 percent, as for two-PSK).

7.3 Effect of autocorrelation function

The effect of the autocorrelation function is illustrated in Fig. 15, which shows the cumulative probability for both autocorrelation functions calculated for a correlation length of 50m, a signaling rate of 16 kb/s, and the switching intervals of 10, 20, and 30m.

As in the two-PSK case, the two autocorrelation functions give nearly the same distribution for a switching interval of 10m. Above this value, the results are similar to those given by two-PSK, except for the positions of the discontinuities. Also, as before, the effect of the correlation length is small.

VIII. EFFECT OF A SWITCHING THRESHOLD

We conclude the study of the $\langle BER \rangle$ degradation by evaluating the effect of adding a threshold condition in the switching tests. The threshold consists of a reference to which the medium-term power $\langle S_j \rangle$ received by the transmitting base station is compared; switching

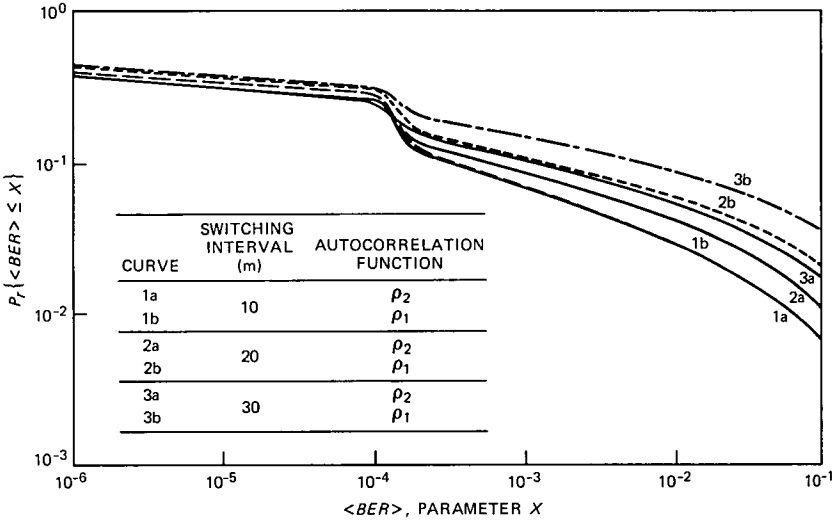

Fig. 15—Same results as in Fig. 12, for four-PSK signals.

is done only if $\langle S_j \rangle$ is smaller than the reference. This condition is added to reduce the switching frequency and thus to decrease the resulting $\langle BER \rangle$ degradation.

The threshold is adjusted relative to the median value of $\langle S_j \rangle$ (in dB) received by the base stations when the mobile unit is at the center of the cell. This quantity is the same for the three base stations.

The simulation was done for four-PSK, the autocorrelation function ρ_2, a decorrelation length of 50m, a switching interval of 10m, and a signaling rate of 16 kb/s. The results are shown in Fig. 16 for the threshold values of 0, −4, and −8 dB, and are compared to the cumulative probability obtained without a threshold for the same parameter values. The comparison shows a significant reduction of the discontinuity caused by switching, but at the cost of degrading the system performance for the $\langle BER \rangle$ values above $\Delta(BER)$. The best compromise is obtained for a threshold of 0 dB.

IX. CONCLUSION

A simple statistical model has been devised for the spatial variations of shadow fading, consisting of a one-parameter spatial autocorrelation function for the log-normal fading loss variable. The shape of the function and the value of the parameter can be varied to emulate different fading conditions in the urban environment. This model was used to simulate shadow fading for a mobile unit moving along a given path in a radio mobile cellular configuration using three-corner base station diversity.

Two significant geometric results emerge from this simulation study. First, the cumulative probability curves for the distance traveled by a mobile unit between consecutive switches, obtained for different fading conditions, can be fitted on the same curves when the distance between switches, and the length of the interval between switching tests are both normalized by the correlation length. Second, the above distribution, the average distance between switches, and the switching frequency are all nearly independent of the path followed by the mobile unit.

The above results were used to evaluate the $\langle BER \rangle$ degradations due to switching, for both two-PSK and four-PSK modulations. We found that, in the worst condition—a mobile unit moving at 55 mph, a decorrelation length equal to a city block, switching tests done every 10m, and a (low) signaling rate of 16 kb/s—the distributions are insignificantly affected by switching for $\langle BER \rangle$ values above 9×10^{-5} for two-PSK, and above 1.5×10^{-4} for four-PSK. These $\langle BER \rangle$ values are found to be about equal to the $\langle BER \rangle$ increment caused by switching for the respective modulation. The cumulative probability roughly doubles below these values. The amplitude of this effect is reduced by increasing the length of the switching test interval, but the improvement is more than canceled by an overall degradation of the cumulative probability distribution.

It was found, as expected, that the switching degradation is reduced when the correlation length increases. The same effect is obtained by

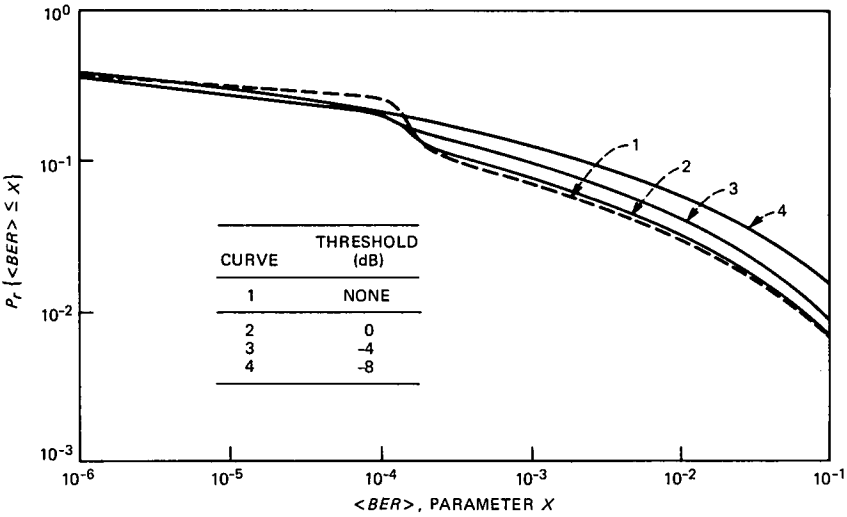

Fig. 16—Cumulative probability of $\langle BER \rangle$ for four-PSK signals, calculated with a threshold switching condition.

using a higher signaling rate or for a mobile unit moving at lower speed (if the switching tests are done at the same intervals).

The addition of a threshold condition in the switching test reduces the amplitude of the discontinuity of the cumulative probability functions. However, this is achieved at the cost of degrading the distribution for large $\langle BER \rangle$. An acceptable compromise between these two effects is obtained for a threshold of 0 dB.

Finally, the $\langle BER \rangle$ statistics are found to be nearly independent of the shape of the autocorrelation function if the switching tests are done at intervals smaller than or equal to 0.2 times the correlation length. Above this value, the results obtained for different shapes diverge increasingly with the length of the interval.

X. ACKNOWLEDGMENT

The author gratefully acknowledges L. J. Greenstein for his many helpful ideas and useful comments.

REFERENCES

1. W. C. Jakes, Jr., Ed., *Microwave Mobile Communication*, New York: Wiley, 1974, Chapters 2 and 5.
2. W. C. Y. Lee and Y. S. Yeh, "On the Estimation of the Second-Order Statistics of Log Normal Fading in Mobile Radio Environment," IEEE Trans. Commun., *COM-22*, No. 6 (June 1974), pp. 869–73.
3. G. D. Ott and A. Plitkins, "Urban Path-Loss Characteristics at 820 MHz," IEEE Trans Veh. Technol., *VT-27*, No. 4 (November 1978), pp. 129–97.
4. Y. S. Yeh and S. C. Schartz, "Outage Probability in Mobile Telephone Due to Multiple Log-Normal Interferers," Globecom '82, Miami, November 1982, pp. 71–98.
5. P. S. Henry and B. Glance, "A New Approach to High-Capacity Digital Mobile Radio," B.S.T.J., *60*, No. 8 (October 1981), pp. 1891–904.
6. D. M. Black and D. O. Reudink, unpublished work.
7. G. Vannucci, "A Digital Carrier Regenerator Applicable to TDMA Satellite Systems," Proc. Int. Symp. on Circuits and Systems, Rome, Italy, May 1982, pp. 1249–52.
8. R. W. Lucky, J. Salz, and E. J. Weldon, Jr., *Principles of Data Communication*, New York: McGraw-Hill, 1968, Chapter 9.

AUTHOR

Bernard S. Glance, Electronic Engineering, 1958, Ecole Speciale de Mechanique et Electricite, Paris, France; Electronic Engineering, 1960, Ecole Superieure d'Electricite, Paris, France; Ph.D. (Electronic Engineering), 1964, Paris University; Thompson, CSF, France, 1958–1966; Varian Associates, 1966–1968; AT&T Bell Laboratories, 1968—. At Thompson, CSF, Mr. Glance researched microwave and millimeter-wave tubes, and at Varian Associates he worked on microwave tube amplifiers. After joining AT&T Bell Laboratories, his initial field of interest was millimeter-wave integrated circuits and RF sources. He subsequently worked on microwave integrated components for use in communications satellites. More recently, he has been involved in analyses and simulations of digital mobile radio systems and point-to-point digital radio systems. Member, IEEE.